

Resolved Spectroscopy of Gravitationally Lensed Galaxies at $z \simeq 2$

Tucker Jones

Department of Physics, University of California, Santa Barbara
Santa Barbara, CA 93106, USA
email: tajones@physics.ucsb.edu

Abstract. Spatially resolved spectroscopy is even more powerful when combined with magnification by gravitational lensing. I discuss observations of lensed galaxies at $z \simeq 2$ with spatial resolution reaching 100 parsecs. Near-IR integral field spectroscopy reveals the kinematics, distribution and physical properties of star forming regions, and gas-phase metallicity gradients. Roughly two thirds of observed galaxies are isolated systems with coherent velocity fields, large velocity dispersion, multiple giant star-forming regions, and negative gas-phase metallicity gradients, suggestive of inside-out growth in gravitationally unstable disks. The remainder are undergoing mergers and have shallower metallicity gradients, indicating mixing of the interstellar gas via gravitational interaction. The metallicity gradients in isolated galaxies are consistent with simulations using standard feedback prescriptions, whereas simulations with enhanced feedback predict shallower gradients. These measurements therefore constrain the growth of galaxies from mergers and star formation as well as the regulatory feedback.

Keywords. galaxies: evolution - galaxies: high-redshift - galaxies: kinematics and dynamics - ISM: abundances - gravitational lensing: strong

1. Introduction

The advent of integral field spectroscopy (IFS) with 8–10 meter telescopes has led to tremendous understanding of the internal structure of high redshift galaxies, particularly at $z \simeq 2 - 3$ where bright nebular emission lines are redshifted to favorable near-infrared wavelengths. Two-dimensional spectral mapping of emission lines reveals the kinematics and distribution of star formation while multiple line ratios can be used to infer the gas-phase metallicity (e.g., Jones *et al.* 2013). However, typical galaxies at $z \gtrsim 2$ are poorly sampled by ground-based instruments, even when using adaptive optics (AO). A promising solution is to observe gravitationally lensed galaxies with high areal magnification factors. Early results showed that lensing can be utilized to achieve physical resolution as fine as 100 pc (Nesvadba *et al.* 2006; Stark *et al.* 2008), and a spectacular example from Jones *et al.* (2013) is shown in Figure 1.

2. Kinematics and Morphology

Samples of lensed galaxies have revealed that a majority of typical galaxies at $z \simeq 2 - 3$ exhibit coherent rotation, while approximately 1/3 are undergoing major mergers (Jones *et al.* 2010a, 2013). These results are consistent with surveys of the most massive galaxies which are sufficiently sampled even without the benefit of lensing (e.g., Förster Schreiber *et al.* 2009). But unlike local disk galaxies, the velocity dispersions are very high in *all* star forming galaxies observed with IFS at $z \gtrsim 2$, typically $\sigma \simeq 50\text{--}100 \text{ km s}^{-1}$ and often exceeding the circular rotation velocity. A further discovery was that nearly all star forming galaxies at $z \gtrsim 2$ are resolved into multiple giant “clumps” of star

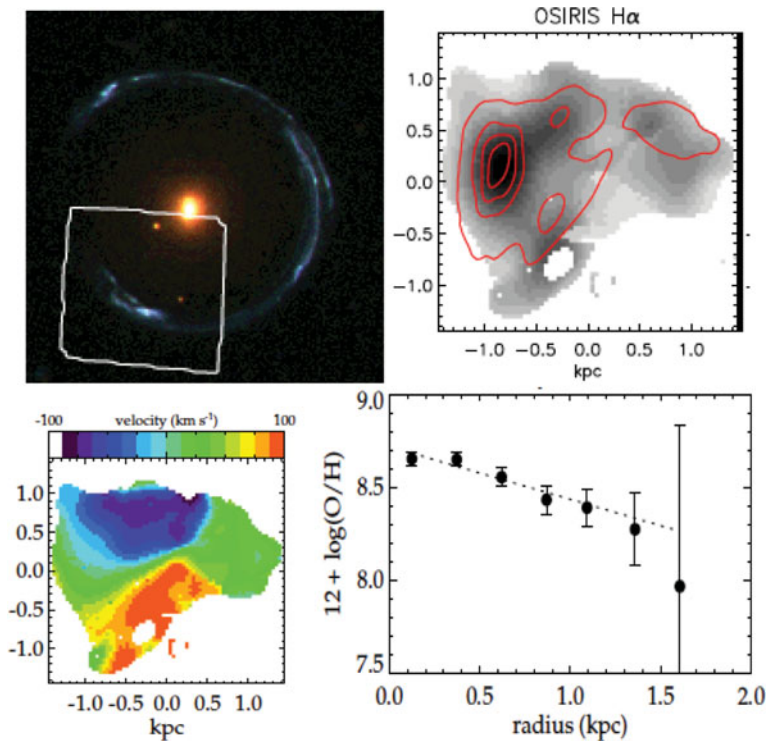


Figure 1. This figure shows an example of the data quality obtained with AO-fed IFS observations of lensed galaxies. *Top left:* HST image of the gravitational lens system SDSS J1148+1930. The blue arc is a star forming galaxy at $z = 2.38$, lensed into a nearly complete Einstein ring. The white box shows the region observed with Keck/OSIRIS and AO. *Top right:* morphology of SDSS J1148+1930, reconstructed in the source plane using the gravitational lens model. Grayscale shows the $H\alpha$ emission and contours show rest-frame UV continuum from HST imaging. Both quantities trace recent unobscured star formation, revealing giant star forming regions with sizes of several hundred parsec. These are also evident as discrete blue clumps of emission in the upper left image, which not be resolved without the combination of gravitational lensing and AO. *Bottom left:* two-dimensional velocity field derived from $H\alpha$ emission centroids in each spatial pixel, reconstructed in the source plane. The galaxy exhibits a regular rotating velocity field with peak-to-peak amplitude $\sim 150 \text{ km s}^{-1}$. *Bottom right:* radial gas-phase metallicity gradient derived from the ratios of strong emission lines ($H\alpha$, $[N \text{ II}]$, $H\beta$, $[O \text{ III}]$). The metallicity is approximately solar in the center, and decreases to $\sim 1/5$ solar in the outer regions.

formation when observed with sufficient spatial resolution (Jones *et al.* 2010a; Livermore *et al.* 2012). Lensing has enabled measurements of their sizes which are found to be comparable to giant H II regions in local starburst galaxies (typically several hundred pc in diameter; Swinbank *et al.* 2009; Jones *et al.* 2010a). Simple calculations show that the kinematic properties and giant clumps are both naturally explained by a scenario in which star formation occurs in gravitationally unstable thick disks: kinematics indicate marginal gravitational instability (with Toomre parameters $Q_T \simeq 1$) which should lead to collapse on scales consistent with observed clump sizes (Genzel *et al.* 2008; Jones *et al.* 2010a). Livermore *et al.* (2012) further demonstrated that the properties of clumps in high redshift galaxies are consistent with the same scaling relations as local star forming disks, given the increased gas fractions (e.g., Tacconi *et al.* 2013). To summarize, the data suggest that a majority of galaxies at $z \simeq 2 - 3$ are evolving in situ with star formation occurring predominantly in gas-rich, gravitationally unstable thick disks.

3. Metallicity Gradients

More recent work has focused on measuring the time evolution of metallicity gradients to constrain models of galaxy evolution. Disk galaxies in the local universe have negative radial gradients in their gas-phase metallicity, with higher metallicities in the central regions (e.g., Vila-Costas & Edmunds 1992). The presence of gradients is explained by inside-out growth of galactic disks, i.e., the disk scale length increases at later times. Evolution of the gradient slope is a sensitive probe of recent dynamical history (e.g., Rupke *et al.* 2010) and of stellar feedback (e.g., Gibson *et al.* 2013; Anglés-Alcázar *et al.* 2014): gravitational interactions and galactic outflows can rapidly redistribute the metal-enriched interstellar medium over large physical scales, flattening any radial gradients.

The first measurement of a metallicity gradient at high redshift found a steep negative slope which would not have been identified without lensing magnification (Jones *et al.* 2010b). Subsequent observations of non-lensed galaxies at $z = 1-4$ have found mostly flat gradients with a significant fraction of positive slopes, but these data may suffer from a number of potential systematic effects related to the metallicity indicators and coarse ~ 5 kpc spatial resolution (Yuan *et al.* 2013). It is clear that $\lesssim 1$ kpc resolution is essential to recover accurate gradients even for large galaxies at $z \simeq 2$, and the best means of achieving this is with lensed galaxies (Yuan *et al.* 2013). Such samples are currently small but are growing rapidly thanks to dedicated efforts with Keck/OSIRIS+AO (Figure 1; Jones *et al.* 2013) and with HST grism spectroscopy via the GLASS survey (Schmidt *et al.* 2014; Jones *et al.* 2014 *in prep*). Figure 2 summarizes the high-resolution measurements presently available. Isolated (non-interacting) lensed galaxies have steeper gradients on average compared to $z \simeq 0$ descendants (Jones *et al.* 2013), in reasonable agreement with cosmological simulations using standard feedback models.

4. Discussion

High resolution measurements of kinematics and star formation are now available for large samples of galaxies at $z \simeq 2$, and their properties are reasonably well explained. However metallicity gradient measurements remain sparse and different samples do not agree. As an example, non-lensed galaxies in Figure 2 have systematically flatter gradients than the lensed sample. This may be due to insufficient spatial resolution, or it could be a real trend induced by selection effects: the non-lensed galaxies are systematically much larger in size which is known to correlate with flatter physical gradient slopes (e.g., Sánchez *et al.* 2014). Larger, reliable samples spanning a range of galaxy properties are clearly needed to understand the evolution of metallicity gradients and the implications for dynamical evolution and feedback. Such samples are within reach of ongoing surveys of lensed galaxies with Keck and HST, and this promises to be an interesting avenue of research in the near future.

Acknowledgements

It is a pleasure to thank the symposium organizers for their effort. This proceeding represents a summary of various work pertinent to the symposium; it would not have been possible without the efforts of numerous collaborators. Readers are referred to the relevant publications for more details: Jones *et al.* (2010a,b, 2013); Schmidt *et al.* (2014); Jones *et al.* (2014 *in prep*), and the references cited here.

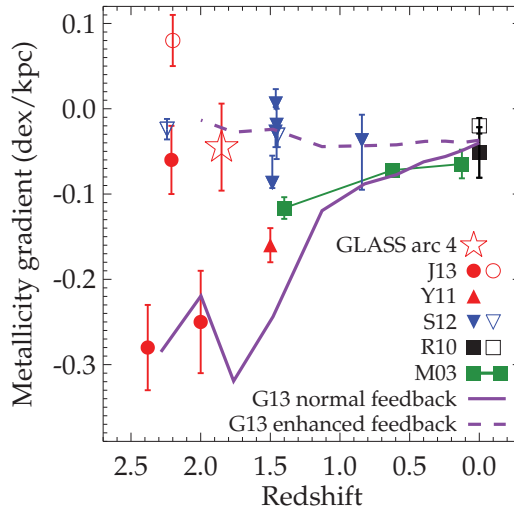


Figure 2. This figure shows the evolution of metallicity gradients with redshift. Measurements of gravitationally lensed galaxies with $\lesssim 300$ pc resolution are shown in red (GLASS arc 4: Jones *et al. in prep*; J13: Jones *et al.* 2013; Y11: Yuan *et al.* 2011), non-lensed galaxies with ~ 1 kpc resolution are shown in blue (S12: Swinbank *et al.* 2012), an average of local gradients are shown in black (R10: Rupke *et al.* 2010), and the Milky Way metallicity gradient evolution measured from planetary nebulae is shown in green (M03: Maciel *et al.* 2003). Solid and hollow symbols denote isolated disks and interacting (or merging) galaxies, respectively, to illustrate that interacting galaxies have flatter gradients on average in the lensed and $z = 0$ samples. We additionally show results of two different feedback schemes in otherwise identical simulations of a galaxy similar to those shown in this figure (G13: Gibson *et al.* 2013). Isolated lensed galaxies at high redshift are more consistent with the “normal” feedback model.

References

- Anglés-Alcázar, D., Davé, R., Özel, F., & Oppenheimer, B. D. 2014, *ApJ*, 782, 84
 Förster Schreiber, N. M., Genzel, R., Bouché, N., *et al.* 2009, *ApJ*, 706, 1364
 Genzel, R., Burkert, A., Bouché, N., *et al.* 2008, *ApJ*, 687, 59
 Gibson, B. K., Pilkington, K., Brook, C. B., Stinson, G. S., & Bailin, J. 2013, *A&A*, 554, A47
 Jones, T. A., Swinbank, A. M., Ellis, R. S., Richard, J., & Stark, D. P. 2010, *MNRAS*, 404, 1247
 Jones, T., Ellis, R., Jullo, E., & Richard, J. 2010, *ApJ*, 725, L176
 Jones, T., Ellis, R. S., Richard, J., & Jullo, E. 2013, *ApJ*, 765, 48
 Livermore, R. C., Jones, T., Richard, J., *et al.* 2012, *MNRAS*, 427, 688
 Maciel, W. J., Costa, R. D. D., & Uchida, M. M. M. 2003, *A&A*, 397, 667
 Nesvadba, N. P. H., Lehnert, M. D., Eisenhauer, F., *et al.* 2006, *ApJ*, 650, 661
 Rupke, D. S. N., Kewley, L. J., & Chien, L.-H. 2010, *ApJ*, 723, 1255
 Sánchez, S. F., *et al.* 2014, *A&A*, 563, A49
 Schmidt, K. B., *et al.* 2014, *ApJ*, 782, L36
 Stark, D. P., Swinbank, A. M., Ellis, R. S., *et al.* 2008, *Nature*, 455, 775
 Swinbank, A. M., Webb, T. M., Richard, J., *et al.* 2009, *MNRAS*, 400, 1121
 Swinbank, A. M., Sobral, D., Smail, I., Geach, J. E., Best, P. N., McCarthy, I. G., Crain, R. A., & Theuns, T. 2012, *MNRAS*, 426, 935
 Tacconi, L. J., Neri, R., Genzel, R., *et al.* 2013, *ApJ*, 768, 74
 Vila-Costas, M. B. & Edmunds, M. G. 1992, *MNRAS*, 259, 121
 Yuan, T.-T., Kewley, L. J., Swinbank, A. M., Richard, J., & Livermore, R. C. 2011, *ApJ*, 732, L14
 Yuan, T.-T., Kewley, L. J., & Rich, J. 2013, *ApJ*, 767, 106